Tokyo Climate Center, Japan Meteorological Agency

TCC News

Autumn 2024

Table of Contents: TCC News No. 78

JMA's Seasonal Numerical Ensemble Prediction for Boreal Winter 2024/2025

This report outlines JMA's dynamical seasonal ensemble prediction for boreal winter 2024/2025 (December – February, referred to as DJF), which was used as a basis for JMA's operational three-month outlook issued on 19 November 2024. The outlook is based on the seasonal ensemble prediction system of the Coupled Atmosphere-ocean General Circulation Model (CGCM).

Summary: Based on output from JMA's seasonal ensemble prediction system, the characteristics of La Niña conditions will be clearer during winter, but will not last until spring. Thus, it is more likely that ENSO-neutral conditions will continue (60%) than the definition of a La Niña event will be met (40%). In association, active convection is expected from the eastern Indian Ocean to the Maritime Continent. Conversely, inactive convection is expected over the western Indian Ocean and the western equatorial Pacific. In the lower troposphere, anti-cyclonic and cyclonic circulation anomalies straddling the equator are expected over the tropical Pacific and from the Indian Ocean to the Maritime Continent, respectively, in association with tropical convection.

1. Sea surface temperature

Figure 1-1 shows predicted SSTs (contours) and related anomalies (shading) for DJF. Negative anomalies are expected from the eastern to central equatorial Pacific, while positive anomalies are expected in the western tropical Pacific and the tropical Indian Ocean, except for some areas of the western part. The cold subsurface water volume increased from the central to eastern equatorial Pacific in October. Output from JMA's seasonal ensemble prediction system suggests that this volume will increase further and propagate eastward. As a result, it is expected that the NINO.3 SST will be below normal by boreal winter. However, these conditions are not expected to last until spring, and the NINO.3 SST is expected to shift nearer to normal toward the coming spring as atmosphere-ocean coupling weakens. In conclusion, La Niña conditions will be clearer during boreal winter but will not last until boreal

spring. Thus, it is more likely that ENSO-neutral conditions will continue (60%) than the definition of a La Niña event will be met (40%).

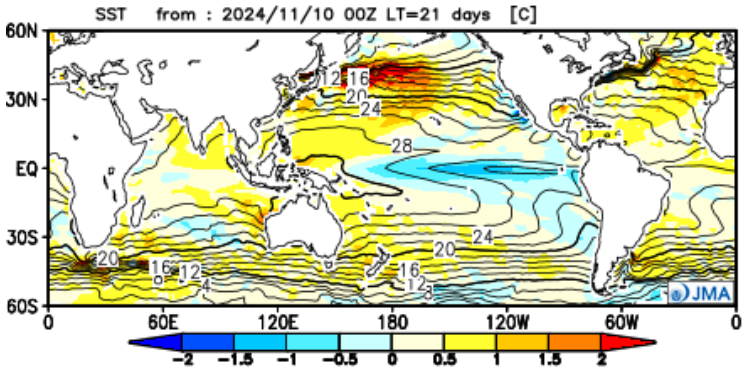

Figure 1-1 Predicted SSTs (contours) and SST anomalies (shading) for December 2024–February 2025 (ensemble mean of 51 members)

2. Prediction for the tropics and sub-tropics

Figure 1-2 (a) shows predicted precipitation (contours) and related anomalies (shading) for DJF. In association with SST anomalies over the tropics, precipitation is expected to be above normal from the eastern Indian Ocean to the Maritime Continent. Conversely, inactive convection is expected over the western equatorial Indian Ocean and the western equatorial Pacific.

Figure 1-2 (b) shows predicted velocity potential (contours) and related anomalies (shading) in the upper troposphere for DJF. In association with the precipitation anomalies described above, negative (i.e., large-scale divergent) anomalies are expected from the eastern Indian Ocean to the Maritime Continent, while positive (i.e., large-scale convergence) anomalies are expected from Africa to the western Indian Ocean and over the western and central Pacific.

Figure 1-2 (c) shows predicted stream functions (contours) and related anomalies (shading) in the upper troposphere for DJF. Anti-cyclonic anomalies (i.e., positive in the Northern Hemisphere) are expected from northern South Asia to East Asia and cyclonic circulation anomalies (i.e., negative in the Northern Hemisphere) straddling the equator are expected over the central tropical Pacific.

Figure 1-2 (d) shows predicted stream functions (contours) and related anomalies (shading) in the lower troposphere for DJF. Anti-cyclonic and cyclonic circulation anomalies straddling the equator are expected over the tropical Pacific and from the Indian Ocean to the Maritime Continent, respectively.

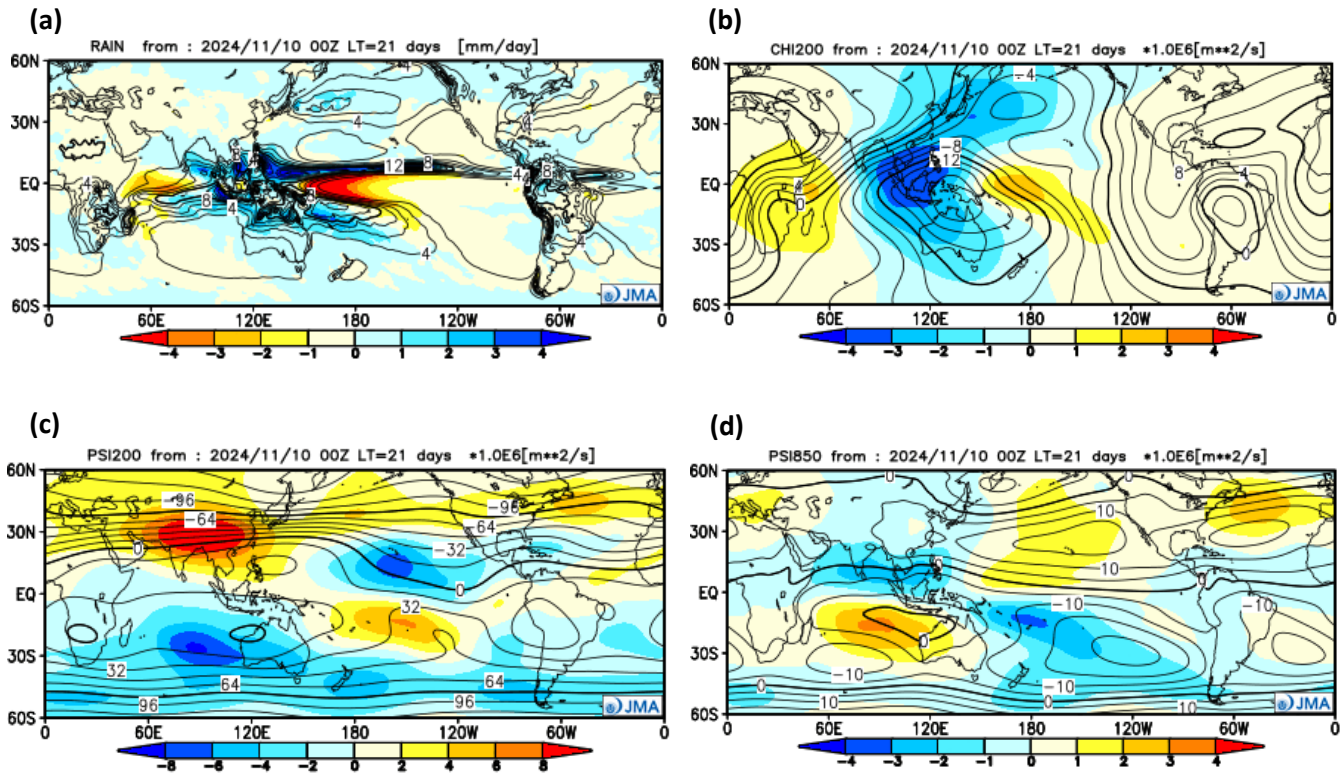

Figure 1-2 Predicted atmospheric fields over 60°N-60°S for December 2024 – February 2025 (ensemble mean of 51 members)

(a) Precipitation (contours) and anomaly (shading). The contour interval is 2 mm/day. (b) Velocity potential at 200-hPa (contours) and anomaly (shading). The contour interval is 2 × 10^6 m^2/s. (c) Stream function at 200-hPa (contours) and anomaly (shading). The contour interval is 16 × 10^6 m^2/s. (d) Stream function at 850-hPa (contours) and anomaly (shading). The contour interval is 5 × 10^6 m^2/s.

3. Prediction for the mid- and high- latitudes of the Northern Hemisphere

Figure 1-3 (a) shows predicted 500-hPa geopotential heights (contours) and related anomalies (shading) for DJF. Positive anomalies are expected over a wide area in the Northern Hemisphere with significantly positive anomalies from the central to eastern Pacific in the mid-latitudes, from eastern North America to the mid-latitude North Atlantic and over Europe. Weak negative anomalies are expected over areas near Japan and parts of the northern North Atlantic.

Figure 1-3 (b) shows predicted sea level pressure (contours) and related anomalies (shading) for DJF. The Iceland Low is expected to be stronger than normal from central to eastern parts. The Aleutian Low is expected to be stronger than normal in the western part and weaker than normal in the eastern part.

(a) (b)

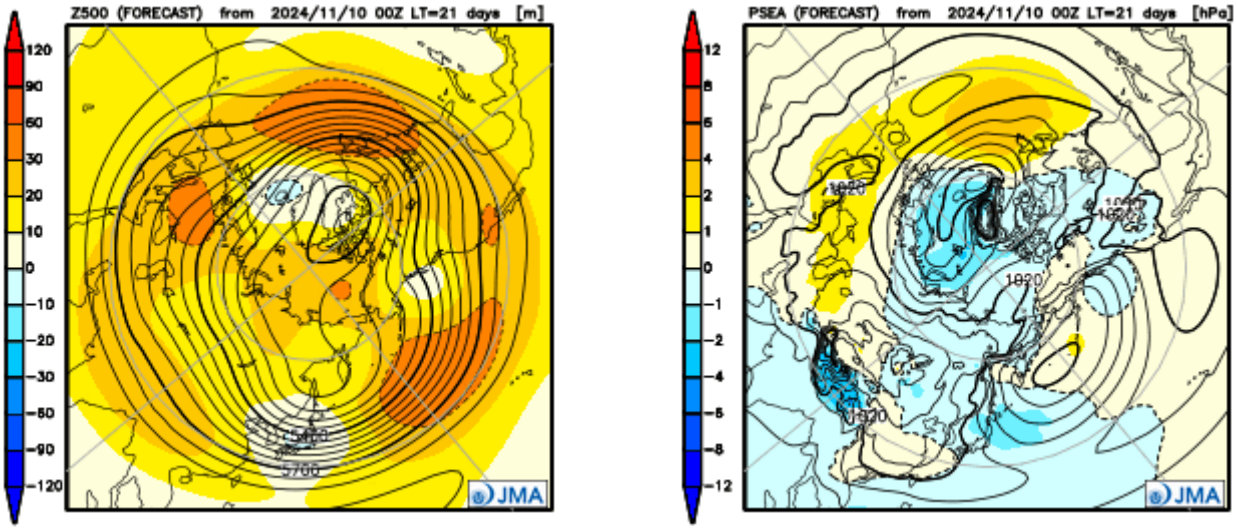

Figure 1-3 Predicted atmospheric fields over the Northern Hemisphere for December 2024 – February 2025 (ensemble mean of 51 members)

(a) Geopotential height at 500-hPa (contours) and anomaly (shading). The contour interval is 60 m. (b) Sea level pressure (contours) and anomaly (shading). The contour interval is 4 hPa.

Note: JMA operates a seasonal Ensemble Prediction System (EPS) using the Coupled atmosphere-ocean General Circulation Model (CGCM) to make seasonal predictions beyond a one-month time range. The EPS produces perturbed initial conditions by means of a combination of the initial perturbation method and the lagged average forecasting (LAF) method. Prediction is made using 51 members from the latest 17 initial dates (3 members are used every day). Details of the prediction system and verification maps based on 30-year hindcast experiments (1991–2020) are available at https://ds.data.jma.go.jp/tcc/tcc/products/model/.

(NAKAMIGAWA Hiroshi, Tokyo Climate Center)

<<Table of contents <Top of this article

Summary of the 2024 Asian Summer Monsoon

This report summarizes the characteristics of the surface climate and atmospheric/oceanographic conditions related to the Asian summer monsoon for 2024.

Note: The Japanese Reanalysis for Three Quarters of a Century (JRA-3Q) dataset (Kosaka et al. 2024) and MGDSST (Kurihara et al. 2006) were used to analyze atmospheric circulation and sea surface temperature (SST) in the research reported here. NOAA Climate Prediction Center (CPC) blended Outgoing Longwave Radiation (OLR) data from the NOAA website (https://ftp.cpc.ncep.noaa.gov/precip/CBO_V1/) were used to infer tropical convective activity. The base period for the normal is 1991 to 2020. The term “anomaly” as used in this report refers to deviation from the normal.

1. Precipitation and temperature

CLIMAT data on total precipitation for the summer monsoon season (June – September) showed more than 140% of the normal in and around Pakistan, in northern Vietnam, and from eastern Mongolia to northern China, while less than 60% of the normal was seen over parts of southern Central Asia (Figure 2-1 (a)). Notably, values exceeding 200% of the normal were seen in and around Pakistan, and it was reported that heavy rain from June to August caused at least 840 fatalities from Bangladesh to Afghanistan (sources: governments of India and Nepal, EM-DAT) and at least 410 fatalities from Nepal to Iran in September (sources: governments of India and Pakistan, European Commission and EM-DAT).

Four-month mean temperatures for the same period were above normal over most of Central, South, Southeast and East Asia, while values were below normal in parts of South and Southeast Asia (Figure 2-1 (b)). In Japan and Korea, summer (June to August) mean temperatures were at record highs since 1898 and 1973 (Korea Meteorological Administration), respectively. In China, monthly mean temperatures were the highest since 1961 for July, August and September (China Meteorological Administration). The summer mean temperature in Hong Kong was the second highest since 1884 (Hong Kong Observatory).

(a) (b)

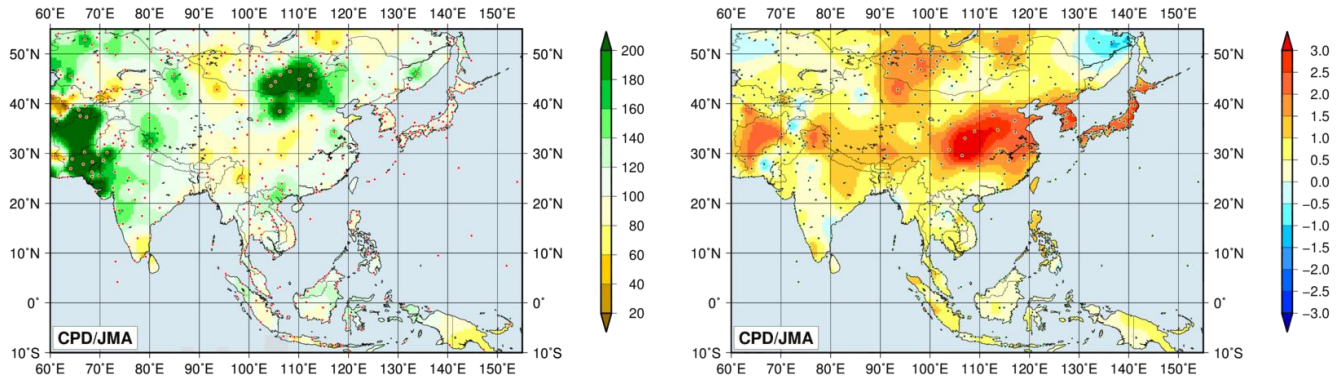

Figure 2-1 Four-month (a) precipitation ratios [%] and (b) mean temperature anomalies [°C] from June to September 2024

The base period for normal is 1991 – 2020. The red (a) and green (b) dots show stations providing map data, which are interpolated due to a lack of CLIMAT reporting and climatological normal values in some areas.

2. Tropical cyclones

There was a total of 18 named tropical cyclones (TCs) over the western North Pacific and the South China Sea by the end of September 2024, compared with the normal of 18.6 (Table 2-1). June to September saw a total of 16 named TCs (climatological normal: 16.1), with 13 approaches or landfalls on Southeast and East Asia and 10 (climatological normal: 9.5) on Japan. Only 4 named TCs had formed by the end of July (climatological normal: 7.9) under suppressed convection in the tropical western North Pacific, similar to post-El Niño summers. However, the total number of named TCs had increased to 18 by the end of September. This striking change was likely due to enhanced convection from the Philippines to the southeast of Japan in August and September, associated with low-level large-scale cyclonic circulations like the monsoon gyre observed in August and frequent intrusions of upper-level high potential vorticity (PV) air masses over warmer ocean waters as described in Section 3.

Table 2-1 Named tropical cyclones over the western North Pacific and the South China Sea by the end of September 2024

Name (number)		Date(UTC)	Category[1)]	Maximum wind[2)] (kt)
Ewiniar	(2401)	25 May - 30 May	TY	75
Maliksi	(2402)	31 May - 31 May	TS	35
Gaemi	(2403)	20 Jul - 26 Jul	TY	90
Prapiroon	(2404)	21 Jul - 23 Jul	STS	55
Maria	(2405)	7 Aug - 12 Aug	STS	55
Son-Tinh	(2406)	11 Aug - 13 Aug	TS	35
Ampil	(2407)	12 Aug - 18 Aug	TY	85
Wukong	(2408)	13 Aug - 15 Aug	TS	35
Jongdari	(2409)	18 Aug - 20 Aug	TS	40
ShanShan	(2410)	21 Aug - 1 Sep	TY	95
Yagi	(2411)	1 Sep - 8 Sep	TY	105
Leepi	(2412)	5 Sep - 6 Sep	TS	35
Bebinca	(2413)	10 Sep - 16 Sep	TY	75
Pulasan	(2414)	15 Sep - 21 Sep	TS	45
Soulik	(2415)	19 Sep -19 Sep	TS	35
Cimaron	(2416)	25 Sep - 26 Sep	TS	35
Jebi	(2417)	27 Sep - 2 Oct	STS	60
Krathon	(2418)	28 Sep - 3 Oct	TY	105

Note: Based on information from the RSMC Tokyo-Typhoon Center.
1) Intensity classification for tropical cyclones.
TS: tropical storm (34 – 47 kt), STS: severe tropical storm (48 – 63 kt), TY: typhoon (≥64 kt)
2) Estimated maximum 10-minute mean wind.
3) Based on early analysis data (rather than best track data) for tropical cyclones from Maria (2405) to Krathon (2418).

3. Monsoon activity and atmospheric circulation

Convective activity inferred from OLR averaged for June – September 2024 (Figure 2-2) was enhanced from the northern Indian Ocean to the Philippines, and was suppressed over a wide area of the tropical western North Pacific except to the southeast of Japan. The anomalous convection observed from the northern Indian Ocean to the tropical western North Pacific was likely a remnant of the El Niño event that lasted until the preceding boreal spring, associated with basin-wide above-normal SSTs in the Indian Ocean (Figure 2-3). OLR index values (Table 2-2) indicate that the overall activity of the Asian summer monsoon (represented by the SAMOI (A) index) was above normal in July and September and below normal in August. The active convection area shifted southwestward from its normal position in most of the period from May to August (see the SAMOI (N) and SAMOI (W) indices), but shifted northeastward in September.

Convective activity in the Asian monsoon region exhibited remarkable intra-seasonal variations. Convection over India and the Bay of Bengal was generally enhanced from mid-May to mid-October, but was suppressed in early August and mid-September (Figure 2-4 (a)). Convection over the Philippines also showed large sub-seasonal

fluctuations (Figure 2-4 (b)), with enhancement in mid-July and from early to mid-September and suppression from June to early July and from late July to August. These intra-seasonal variations were probably related to boreal summer intra-seasonal oscillation (BSISO; Lee et al. 2013; Kikuchi 2021). In July and September, enhanced convection migrated northwestward from the western equatorial Pacific to the Philippines, followed by an intensified Pacific-Japan (PJ) pattern (Nitta 1987, Kosaka and Nakamura 2006), and was possibly related to a series of TC occurrences.

Figure 2-5 shows four-month mean 200- and 850-hPa stream function fields for June – September. In the upper troposphere (Figure 2-5 (a)), the northeastward extension of the Tibetan High was intensified, resulting in a record hot summer in East Asia as described in Section 1. Such upper-level conditions may be attributable to the Silk Road teleconnection (Enomoto 2003), manifested as a wavy-like anomaly pattern along the subtropical jet stream over Eurasia, as well as enhanced convection in the Asian monsoon region (Figure 2-2). Upper-level anticyclonic and cyclonic circulation anomalies were seen to the east and southeast of Japan, respectively. This pair of anomalies is indicative of frequent appearance of Rossby-wave breaking, and thus upper-level high-PV air masses detached from the mid-Pacific trough (Figure 2-6). These masses migrated toward the southeast of Japan, contributing to enhanced convection and possibly enhanced TC generation in August and September via dynamically induced ascent. Enhanced convection to the southeast of Japan also reinforced upper-level anticyclonic circulation anomalies to the east of Japan, which may be viewed as positive feedback (Takemura and Mukougawa 2020a, 2020b).

In the lower troposphere (Figure 2-5 (b)), the North Pacific Subtropical High (NPSH) anomalously extended westward to areas such as Japan and the Philippines, contributing to intense hot conditions over a wide area of East Asia from July through September. This enhanced extension may be partly attributable to active cumulus convection from the northern Indian Ocean to the Philippines (Figure 2-2). Compared with the characteristics of post-El Niño summers (Xie et al. 2016), the enhanced southwestward extension of the NPSH during this summer was consistent, but its intensification over and around Japan notably differed.

The above-normal temperatures observed in most Asian regions (Figure 2-1(b)) were underpinned by unprecedentedly high tropospheric temperatures over the mid-latitudes of the Northern Hemisphere and the tropics, where anomalies exceeded 3 – 4 standard deviations of interannual variations (Figure 2-7). These extremely high temperatures were due to the lingering effects of the El Niño event terminating in the proceeding boreal spring and other factors, as well as a long-term increasing trend associated with global warming.

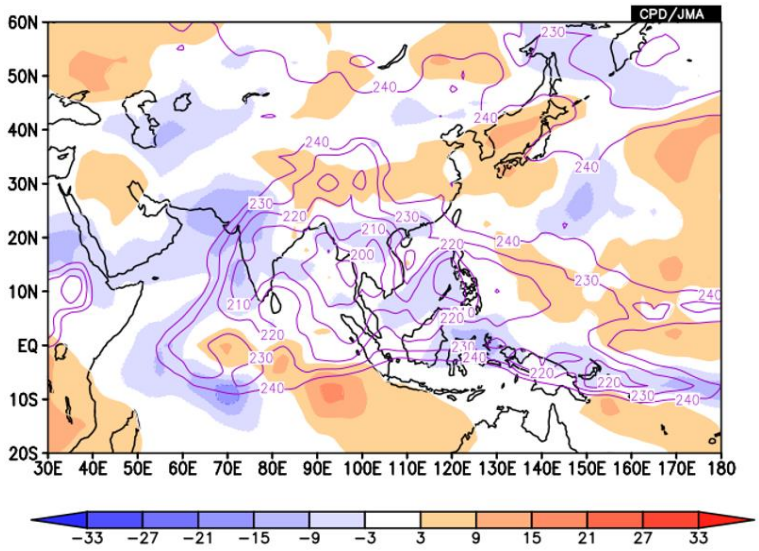

Figure 2-2 Four-month mean OLR [W/m^2] for June–September 2024
Contours indicate OLR lower than 240 W/m^2 at intervals of 10 W/m^2, and color shading denotes OLR anomalies from the normal (i.e., the 1991–2020 average). Negative (cold color) and positive (warm color) OLR anomalies show enhanced and suppressed convection compared to the normal, respectively.

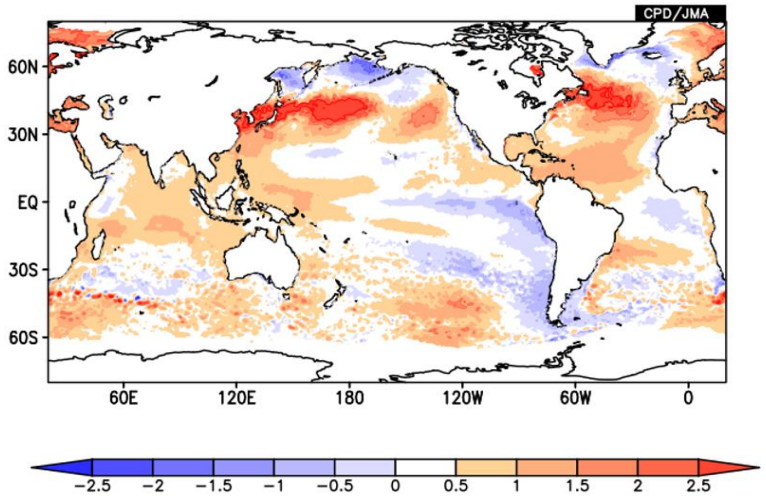

Figure 2-3 Four-month mean SST anomalies [°C] for June–September 2024
The base period for the normal is 1991 – 2020.

Table 2-2 Summer Asian Monsoon OLR Index (SAMOI) values observed from May to September 2024
Asian summer monsoon OLR indices (SAMOI) are derived from OLR anomalies. SAMOI (A), (N) and (W) indicate the overall activity of the Asian summer monsoon, its northward shift and its westward shift, respectively. SAMOI definitions are as follows: SAMOI (A) = (-1) × (W + E); SAMOI (N) = S – N; SAMOI (W) = E – W. W, E, N and S indicate area-averaged OLR anomalies for the respective regions shown in the figure on the right normalized by their standard deviations.

	Summer Asian Monsoon OLR Index (SAMOI)		
	SAMOI (A): Activity	SAMOI (N): Northward-shift	SAMOI (W): Westward-shift
May 2024	-0.2	-0.3	+0.7
Jun 2024	-0.1	-0.4	+0.4
Jul 2024	+0.8	-0.4	-0.1
Aug 2024	-1.3	-1.0	+1.1
Sep 2024	+0.9	+1.8	-0.5

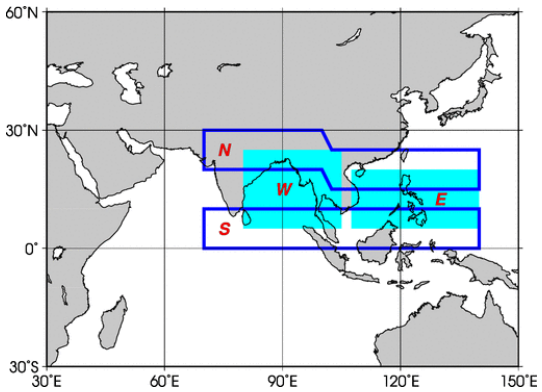

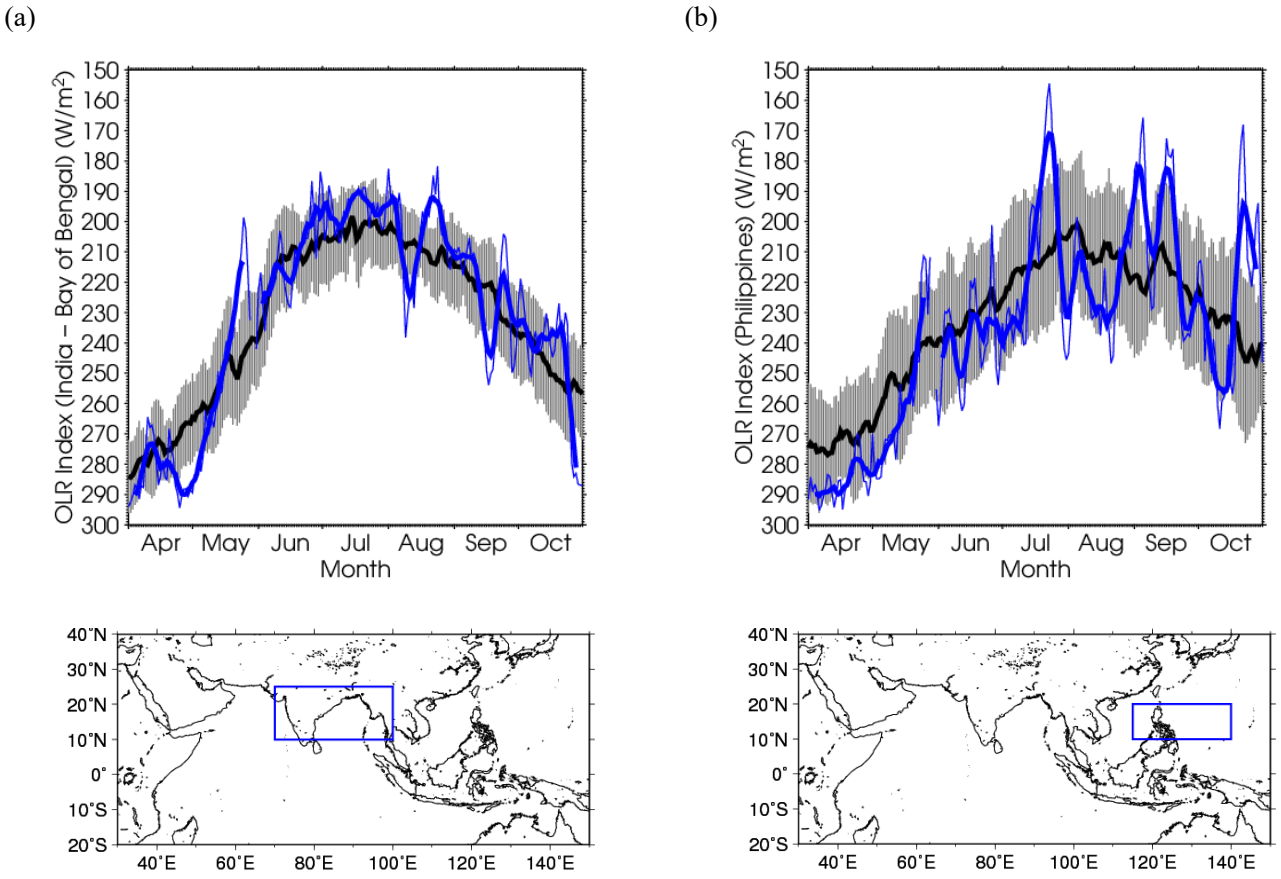

Figure 2-4 Time-series representation of OLR [W/m^2] averaged over (a) India and the Bay of Bengal (shown by the rectangle on the bottom: 10°N - 25°N, 70°E - 100°E) and (b) the Philippines (shown by the rectangle on the bottom: 10°N - 20°N, 115°E - 140°E) during a period from April to October 2024

The OLR indices are calculated after Wang and Fan (1999). The thick and thin blue lines indicate seven-day running mean and daily mean values, respectively. The black line denotes the normal (i.e., the 1991 - 2020 average), and the gray shading shows the range of the standard deviation calculated for the time period of the normal.

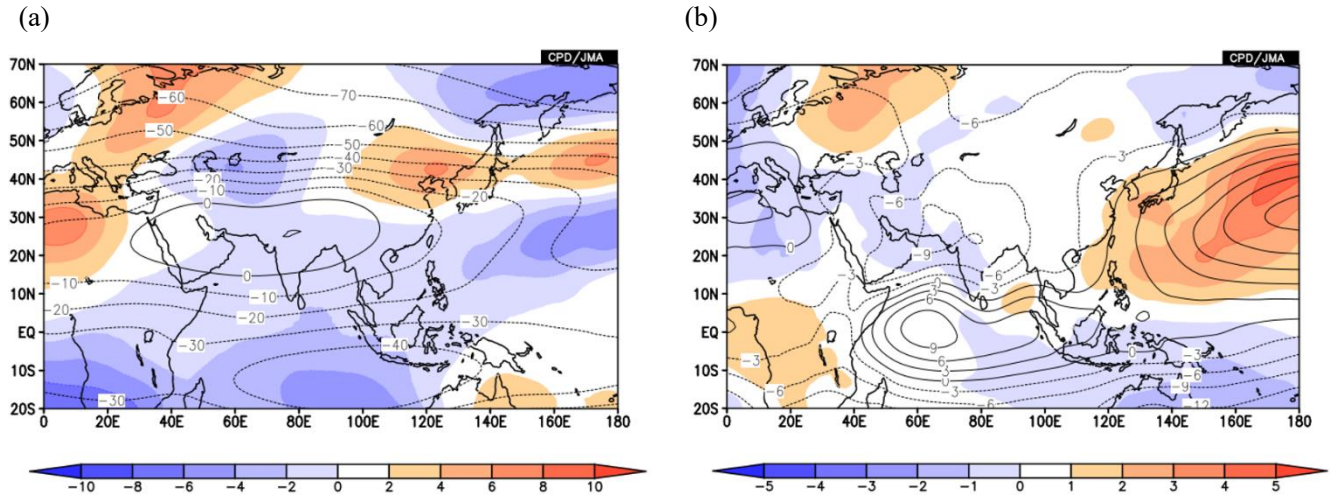

Figure 2-5 Four-month mean (a) 200-hPa and (b) 850-hPa stream function [10^6 m^2/s] for June–September 2024

Contours indicate stream function at intervals of (a) 10 × 10^6 m^2/s and (b) 3 × 10^6 m^2/s, and shading shows stream function anomalies. Red (blue) shading denotes anti-cyclonic (cyclonic) circulation anomalies in the Northern Hemisphere, and vice-versa in the Southern Hemisphere. The base period for the normal is 1991 – 2020.

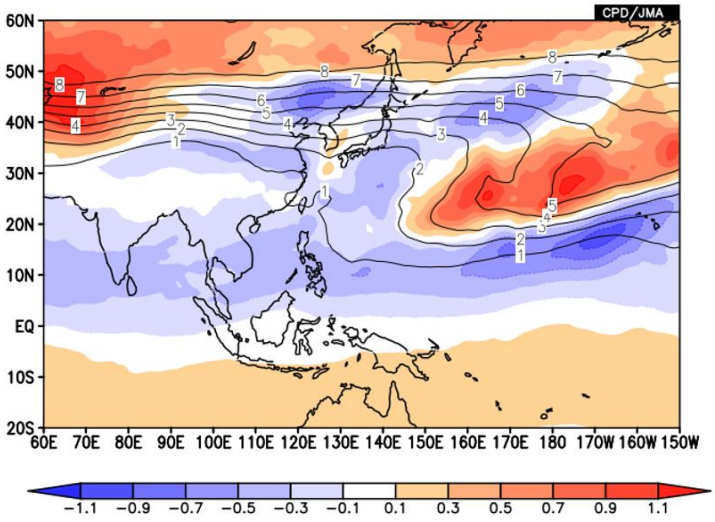

Figure 2-6 Four-month mean 360-K isentropic potential vorticity [PVU; $10^{-6}m^2s^{-1}K\ kg^{-1}$] for June–September 2024
Shading indicates anomalies, and contours show potential vorticity at intervals of 1 PVU. The base period for the normal is 1991 – 2020.

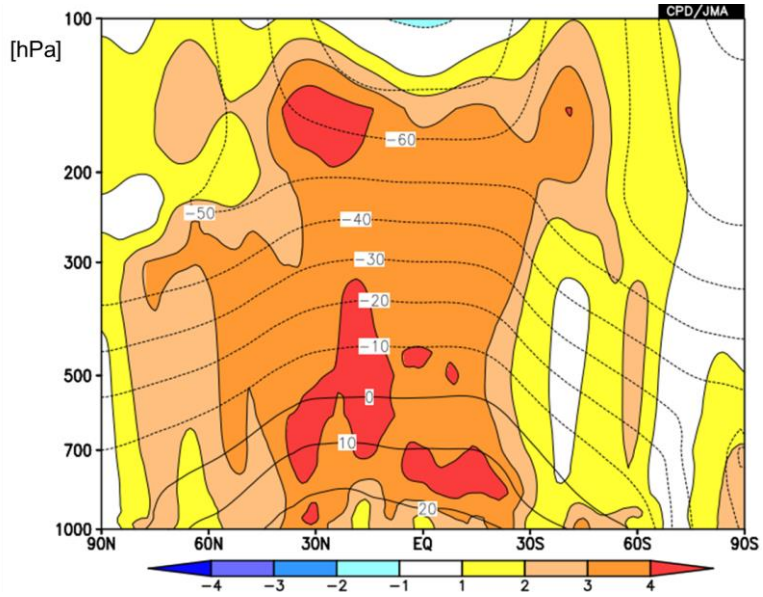

Figure 2-7 Latitude-height cross section of zonal mean temperature [°C] and normalized anomaly for June-September 2024
The contours indicate temperature at intervals of 10°C. The shading indicates normalized temperature anomalies by local standard deviation of interannual variations. The base period for the normal is 1991 – 2020.

References

Enomoto, T., B. J. Hoskins and Y. Matsuda, 2003: The formation mechanism of the Bonin high in August. *Quart. J. Roy. Meteor. Soc.*, **129**, 157–178.

Kikuchi, K., 2021: The boreal summer intraseasonal oscillation (BSISO): A review. *J. Meteor. Soc. Japan*, **99**, 933-972.

Kosaka, Y., and H. Nakamura, 2006: Structure and dynamics of the summertime Pacific-Japan teleconnection pattern. *Quart. J. Roy. Meteor. Soc.*, **132**, 2009-2030.

Kosaka Y., S. Kobayashi, Y. Harada, C. Kobayashi, H. Naoe, K. Yoshimoto, M. Harada, N. Goto, J. Chiba, K. Miyaoka, R. Sekiguchi, M. Deushi, H. Kamahori, T. Nakaegawa; T. Y. Tanaka, T. Tokuhiro, Y. Sato, Y. Matsushita, K. Onogi, 2024: The JRA-3Q Reanalysis. *J. Meteor. Soc. Japan*, **102**, 49-149. https://doi.org/10.2151/jmsj.2024-004

Kurihara, Y., T. Sakurai, and T. Kuragano, 2006: Global daily sea surface temperature analysis using data from satellite microwave radiometer, satellite infrared radiometer and in-situ observations. *Weather Service Bulletin*, **73**, Special issue, s1-s18 (in Japanese).

Lee, J.-Y., B. Wang, M. C. Wheeler, X. Fu, D. E. Waliser, and I.-S. Kang, 2013: Real-time multivariate indices for the

boreal summer intraseasonal oscillation over the Asian summer monsoon region. *Clim. Dyn.*, **40**, 493-509.

Nitta, T., 1987: Convective activities in the tropical western Pacific and their impact on the Northern Hemisphere summer circulation. *J. Meteor. Soc. Japan*, **65**, 373-390.

Takemura, K, and H. Mukougawa, 2020a: Dynamical Relationship between Quasi-stationary Rossby Wave Propagation along the Asian Jet and Pacific-Japan Pattern in Boreal Summer. *J. Meteor. Soc. Japan*, **98**, 169-187.

Takemura, K, and H. Mukougawa, 2020b: Maintenance Mechanism of Rossby Wave Breaking and Pacific-Japan Pattern in Boreal Summer. *J. Meteor. Soc. Japan*, **98**, 1183-1206.

Wang, B. and Z. Fan, 1999: Choice of South Asian summer monsoon indices. *Bull. Amer. Meteor. Soc.*, **80**, 629–638.

Xie, S.-P., Y. Kosaka, Y. Du, K. Hu, J. S. Chowdary and G. Huang, 2016: Indo-Western Pacific Ocean Capacitor and Coherent Climate Anomalies in Post-ENSO Summer: A Review. *Adv. Atmos. Sci.*, **33**, 411-432.

(SATO Hirotaka, Tokyo Climate Center)

<<Table of contents <Top of this article

Status of the Antarctic Ozone Hole in 2024

The onset of the Antarctic ozone hole in 2024 was later than the most recent decadal average due to a small low-temperature area in the stratosphere, while its annual maximum size matched the average.

Since the early 1980s, the Antarctic stratospheric ozone level has fallen every year in austral spring with a peak in September or early October. This area of depletion is referred to as the Antarctic ozone hole.

JMA analysis based on data from the Ozone Mapper Profiler Suite (OMPS) on board the Suomi National Polar-orbiting Partnership (NPP) satellite indicates that the 2024 Antarctic ozone hole appeared in mid-August and expanded from late August, which was later than 2023 and the most recent decadal average. The scale of the hole was subsequently close to the average in September (Figure 3-1, upper left). Its annual maximum size (observed on 28 September) was 22.4 million square kilometers, equivalent to 1.6 times the size of Antarctica (Figure 3-1, upper right). This was close to the average of the most recent decade but smaller than that of 2023. In July and August 2024 the polar vortex over Antarctica was unstable, and the low-temperature area in the stratosphere was smaller than that of the recent decadal average and 2023. As a result, formation of polar stratospheric clouds (PSCs), which plays an important role in ozone depletion, was suppressed, and the start of ozone hole expansion was delayed. In September the low-temperature area expanded to the same level as the most recent decadal average, and the maximum ozone hole area was close to the average.

As an overall trend, the annual maximum size of the Antarctic ozone hole is very likely to have decreased since 2000 (statistically significant at a confidence level of 90%).The *WMO/UNEP Scientific Assessment of Ozone Depletion: 2022* reports that total column ozone in the Antarctic continues to recover, notwithstanding substantial interannual variability in the size, strength and longevity of the ozone hole, and is expected to return to 1980 values around 2066.

The ozone layer acts as a shield against ultraviolet radiation, which can cause skin cancer. The Antarctic ozone hole was first recognized in the early 1980s, and large-scale events have been observed since the 1990s. Its maximum area on record was 29.8 million square kilometers (2000). Antarctic ozone depletion caused an expansion of the tropics and a poleward shift of the jet stream and storm tracks in the Southern Hemisphere that led to pronounced changes in summertime surface climate conditions according to recent assessment.

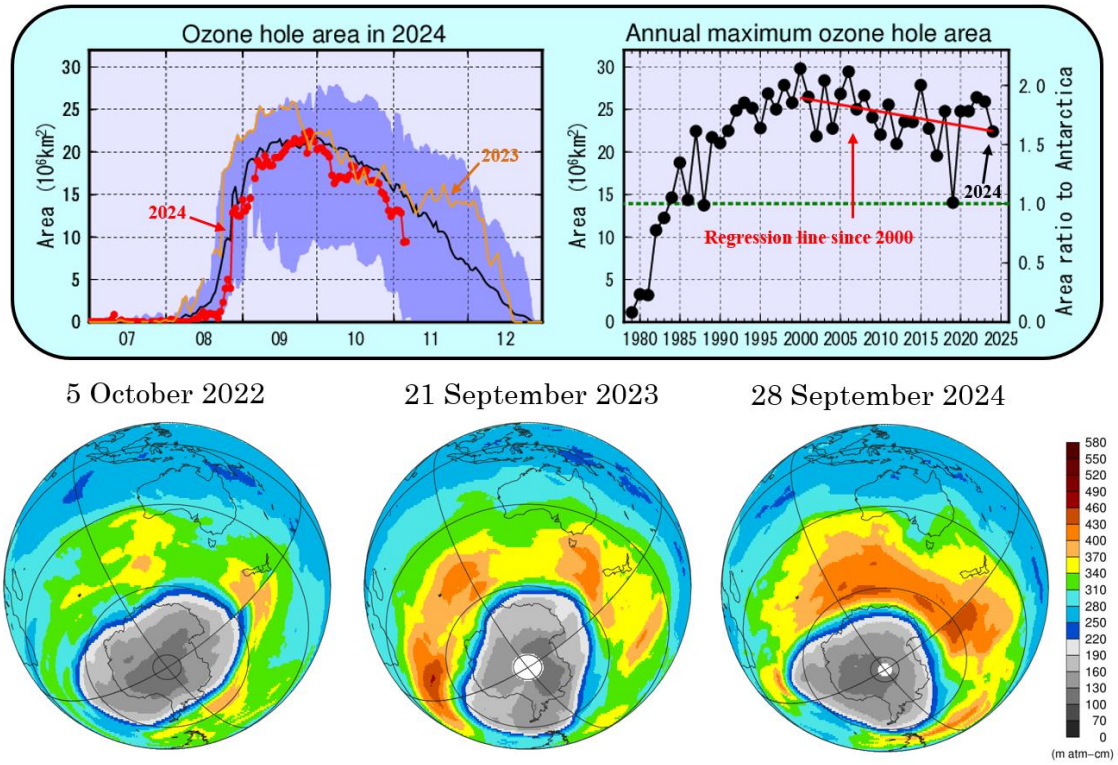

Figure 3-1 Antarctic ozone hole observation

Upper left: Time-series representation of the daily ozone hole area for 2024 (red line), 2023 (orange line) and the 2014 – 2023 average (black line). Blue shading represents the range of daily maxima and minima over the previous 10 years. JMA defines the extent of Antarctic ozone hole expansion area expanding as the area in which the total ozone column value is less than or equal to 220 m atm-cm.

Upper right: Inter-annual variability of the annual maximum ozone hole area. The green dotted line shows the area of the Antarctic Continent (13.9 million square kilometers).

Bottom: Snapshots of total column ozone distribution on the day of the annual maximum ozone hole area for the previous three years; the Antarctic ozone hole is shown in grey. Images are based on NASA satellite data.

(SUZUKI Takashi, Atmospheric Environment and Ocean Division)

<<Table of contents <Top of this article

Status of the Arctic Sea Ice in 2024

It is virtually certain that there has been a long-term decreasing trend of sea ice extent in the Arctic Ocean since 1979, when the current method of monitoring using satellite sensors began. The trend is statistically significant at a confidence level of 99%. The reduction in the annual minimum extent is particularly notable at 0.085 × 10^6 km^2 per year up to 2024 (Figure 4-1).

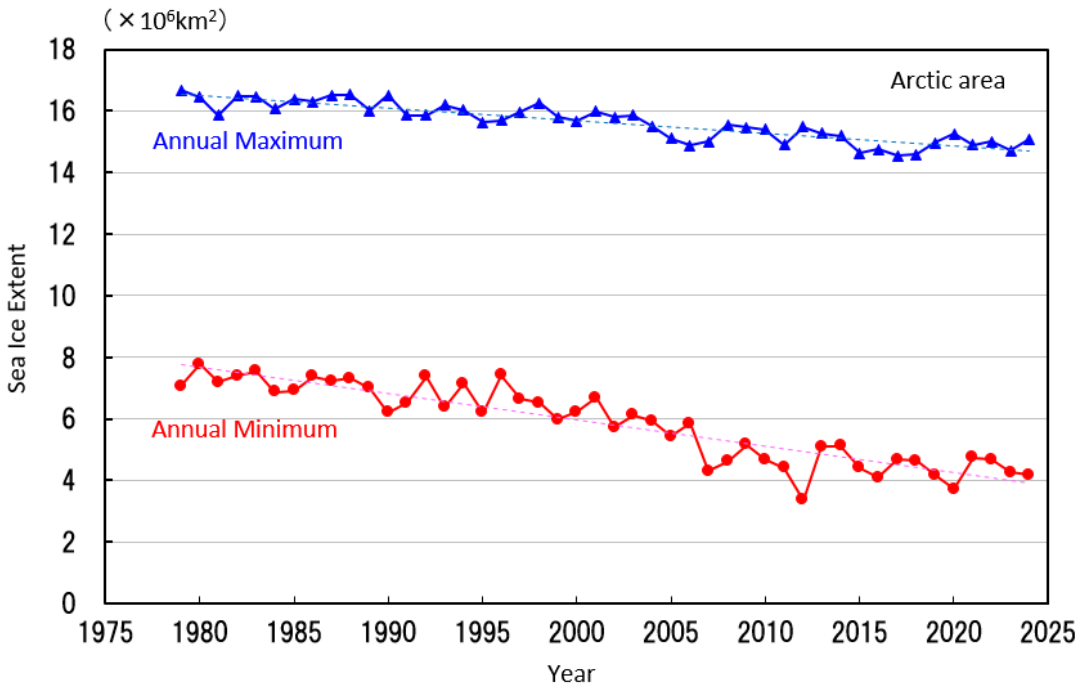

Figure 4-1Time-series representations of annual maximum and annual minimum sea ice extent in the Arctic Ocean (including the Sea of Okhotsk and the Bering Sea) from 1979 to 2024
Blue and red lines indicate annual maximum and annual minimum sea ice extents, respectively, with dashed lines indicating linear trends. Sea ice extents are calculated from brightness temperature data provided by NASA (the National Aeronautics and Space Administration) and NSIDC (the National Snow and Ice Data Center).

Based on preliminary analysis, the annual maximum Arctic sea ice extent was 15.08 × 10 ^{6} km^{2} on 10 March 2024, marking the 12th-lowest value since 1979. The value subsequently decreased during spring and summer in the Northern Hemisphere and reached its annual minimum of 4.18 × 10 ^{6} km^{2} on 6 September, marking the 4th-lowest level since 1979 (Figure 4-2, 4-3).

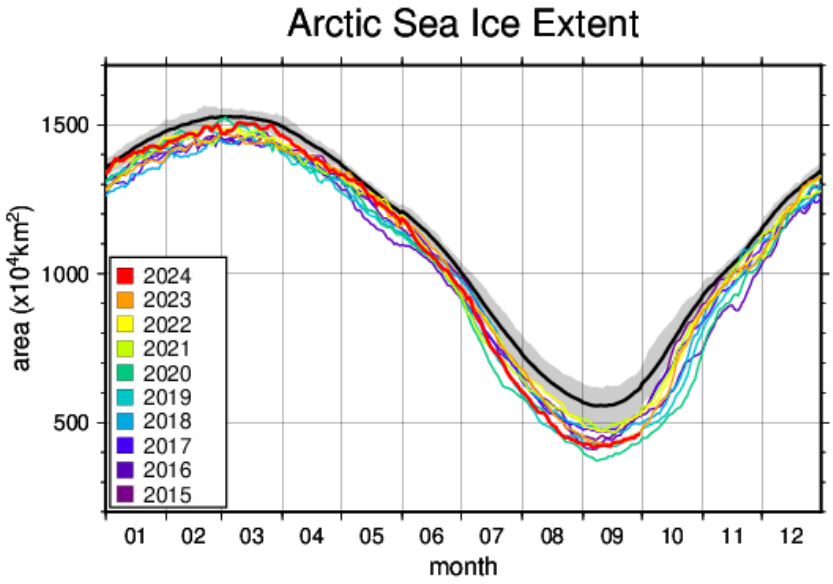

Figure 4-2 Annual variations in the Arctic sea ice extent
The black lines represents the normal, and shading represents the normal range. The base period for the normal is 1991 – 2020.

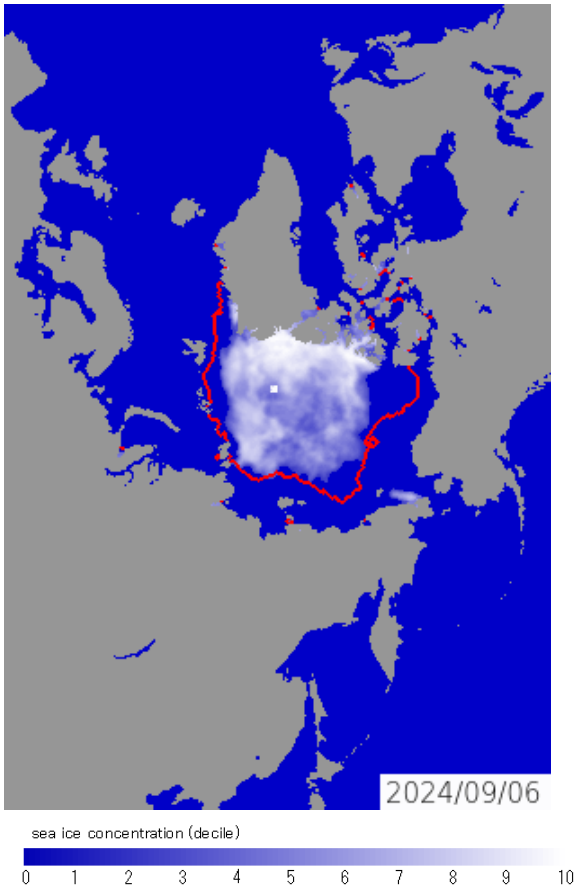

Figure 4-3 Annual minimum Arctic sea ice distribution
As of 6 September 2024. The red lines represents the normal extent. The base period for the normal is 1991 – 2020.

*(*HAMADA Keiji*, Office of Marine Prediction)*

<<Table of contents <Top of this article

Climate characteristics and factors behind extremely high temperatures from July onward and heavy rainfall in late July 2024

Record-high temperatures were observed nationwide in Japan in July 2024, with the national average even exceeding the previous July 2023 record. This persisted into August, with unprecedented temperatures in western Japan. Heavy rainfall was observed in northern Japan in late July, with the second-highest-ever levels on the Sea of Japan side.

TCC issued a press release regarding climate characteristics and factors behind extremely high temperatures from July onward and heavy rainfall in late July 2024. It summarized discussions by the JMA Advisory Panel on Extreme Climatic Events (comprised of prominent climate science academics and researchers) held on 2 September 2024 to identify possible causative factors behind the extreme summer meteorological conditions.

From the press release, the factors behind the extremely high temperatures observed from July onward can be summarized as follows (Figure 5-1):

- The subtropical jet stream (STJ) persistently meandered northward near Japan. Areas of western Japan and elsewhere were covered by a warm high extending into the upper troposphere.
- In July the North Pacific Subtropical High (NPSH) was persistently enhanced south of Japan and extended to

western parts of the country. This may be attributable to active cumulus convection over the northern Indian Ocean.

- In addition to enhanced solar radiation in the high-pressure area, temperatures rose with downward motion.
- Sea surface temperatures (SSTs) around Japan were extremely higher than normal.
- In addition to long-term global warming, temperatures in the mid-latitudes of the Northern Hemisphere were record high due to an El Niño event that continued until spring and other factors.

The factors behind heavy rainfall over northern Japan in late July and global warming effects on these extreme events are also examined.

The press release is available at https://www.data.jma.go.jp/tcc/data/news/press_20241018.pdf.

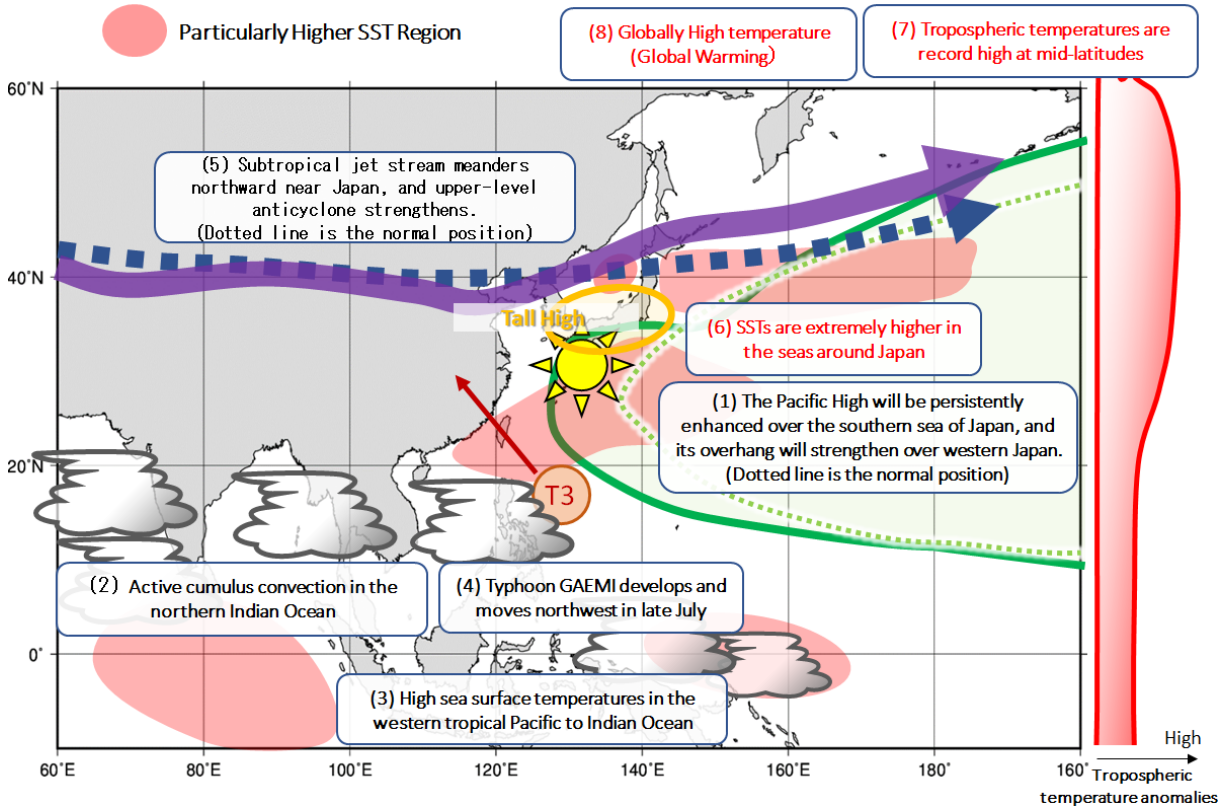

Figure 5-1 Large-scale atmospheric flow producing extremely high temperatures in July

(TAKAHAHI, Kiyotoshi, Tokyo Climate Center)

<<Table of contents <Top of this article

TCC and WMC Tokyo co-contributions to Regional Climate Outlook Forums in Asia

WMO Regional Climate Outlook Forums (RCOFs) bring together national, regional and international climate experts on an operational basis to produce regional climate outlooks based on inputs from participating NMHSs, regional institutions, Regional Climate Centres (RCCs) and global producers of climate predictions. By providing a platform for countries with similar climatological characteristics to discuss related matters, these forums ensure consistency in terms of access to and interpretation of climate information. In spring 2024, TCC and WMC (World Meteorological Centre) Tokyo experts participated in the following two RCOFs in Asia.

- The 29th winter session of the South Asian Climate Outlook Forum (SASCOF-29)
- The 12th session of the East Asia winter Climate Outlook Forum (EASCOF-12)

1. SASCOF-29

The 29th winter session of the South Asian Climate Outlook Forum (SASCOF-29) and Climate Services User Forum (CSUF) was hosted online by RCC-Pune on 25, 26 September and 3 October.

At the event, WMC Tokyo representatives provided winter outlooks based on climate monitoring and forecast products from the TCC website, highlighting Copernicus Climate Change Service (C3S) multi-model ensemble prediction incorporating JMA's seasonal prediction system. It was reported that La Niña conditions would develop by boreal winter (60%).

In the session titled IV: Improvements and Updates in Seasonal Forecasts, a TCC expert reported on the seasonal tropical cyclone (TC) forecast over the western north Pacific, which started experimentally in May 2024, and contributed to discussions on seasonal TC forecasts.

2. EASCOF-12

The 12th Session of the East Asia winter Climate Outlook Forum (EASCOF-12) was hosted by the Korea Meteorological Administration (KMA) in Daejeon in Korea from 6 to 8 November 2024. Around 50 experts from China, Japan, the Republic of Korea and Mongolia attended to review the latest summer and recent climatic characteristics (session 1), the current status and future plans associated with climate services and technology (session 2), and the seasonal outlook for winter 2024/2025 (session 3). Two TCC experts gave presentations on recent climate features in Japan (session 1), recent updates on TCC services and activities (session 2), and the seasonal outlook for winter 2024/2025 over Japan (session 3). These exchanges of expertise are expected to help develop understanding of phenomena related to the East Asian climate and support improvement of associated climate services.

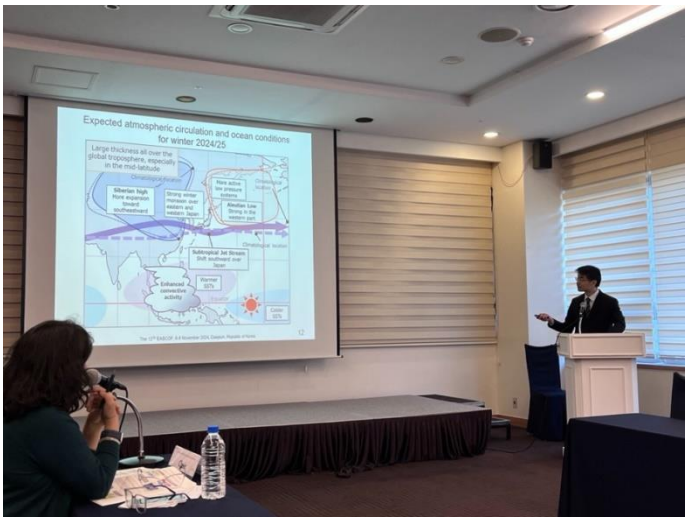

TCC expert (Mr. KAZAMA)'s presentation in EASCOF-12

(SASCOF-29:TAKAHASHI Kiyotoshi, EASCOF-12:KAZAMA Chihiro and KATO Nariko, Tokyo Climate Center)

<<Table of contents <Top of this article

TCC contribution to 6th WCRP international Conference on Reanalysis

The Sixth WCRP International Conference on Reanalysis (ICR6: https://icr6.climcore.org/) was held in Tokyo from 28 October to 1 November 2024 under initiatives from the World Climate Research Programme (WCRP), the Japan Meteorological Agency (JMA), Climate change actions with co-creation powered by Regional weather information and E-technology (ClimCORE), and The University of Tokyo. More than 200 experts from 30 countries and regions came together to discuss state-of-the-art production techniques and utilization for global and regional reanalysis data.

At the conference's poster session, staff from the Tokyo Climate Center (TCC) gave a presentation titled Utilization of Reanalysis in Japan Meteorological Agency -focusing on its application.

The presentation highlighted a wide range of utilization for JMA Reanalysis (JRA-3Q, https://jra.kishou.go.jp/JRA-3Q/index_en.html) in actual operation, from climate analysis to WDCGG CO^2 back-trajectory analysis. Particular focus was placed on TCC activities such as provision of various products, a powerful web-based tool for climate system analysis (iTacs) and social application through the JMA Advisory Panel on Extreme Climatic Events (comprised of prominent climate science academics and researchers).

(TAKAHAHI Kiyotoshi, Tokyo Climate Center)

<<Table of contents <Top of this article

You can find the latest newsletter from the Japan International Cooperation Agency (JICA).

JICA Magazine

https://jicamagazine.jica.go.jp/en/

"JICA magazine" is a public relations magazine published by JICA. It introduces the current situations of developing countries around the world, the people who are active in the field, and the content of their activities.

Any comments or inquiry on this newsletter and/or the TCC website would be much appreciated.
Please e-mail to tcc@met.kishou.go.jp.
(Editors: HARADA Masashi, TAKAHASHI Kiyotoshi)

Tokyo Climate Center, Japan Meteorological Agency
3-6-9 Toranomon, Minato City, Tokyo 105-8431, Japan

TCC Website:
https://ds.data.jma.go.jp/tcc/tcc/index.html